Journal of Magnetism and Magnetic Materials 646 (2026) 173986

Contents lists available at ScienceDirect

Journal of Magnetism and Magnetic Materials

journal homepage: www.elsevier.com/locate/jmmm

The vacancy-induced magnetism of MgO single crystals and its role in the measurement of the magnetic properties of atomically thin films

Iban Llamas [a], José Luis Fernández-Cuñado [a,b,c], Cristina Navío [a], Pilar Marín [d,e], Patricia de la Presa [d,e], Rodolfo Miranda [a,b,c,*], Antonio Hernando [a,d,f,*]

[a] IMDEA Nanociencia, 28049 Madrid, Spain
[b] Departamento de Física de la Materia Condensada, Universidad Autónoma de Madrid, 28049 Madrid, Spain
[c] Instituto de Ciencia de Materiales Nicolás Cabrera, Universidad Autónoma de Madrid, 28049 Madrid, Spain
[d] Instituto de Magnetismo Aplicado, 28049 Madrid, Spain
[e] Departamento de Física de Materiales, Universidad Complutense de Madrid, 28049 Madrid, Spain
[f] Donostia International Physics Center, San Sebastián, Spain

ARTICLE INFO

Keywords:
d^0 ferromagnetism
MgO
FeNi films
Proton irradiation
SQUID
MOKE

ABSTRACT

Although bulk oxide substrates are typically diamagnetic, they can develop d^0 ferromagnetism. MgO single crystals are often used as substrates for the growth of ultrathin magnetic films and superlattices assuming that their behavior is perfectly diamagnetic. We demonstrate here, however, that even highly perfect MgO(001) single crystals can display a SQUID ferromagnetic signal that, although small, can mask completely the signal coming from atomically-thin magnetic films grown on them. Our characterization of pristine MgO single crystals revealed the existence of paramagnetic clusters of magnetic impurities in the bulk with a density of 5.13×10^{18} clusters/cm^3 and an average magnetic moment of 5.85 μ_B, which generate strong paramagnetism at 5 K. In addition, the MgO single crystals show ferromagnetism at 300 K with very small saturation magnetization of 3×10^{-3} emu/cm^3, coercive fields of the order of 100 Oe and remanence 5×10^{-4} emu/cm^3, related to composite Mg and oxygen vacancies in the surface region, which persist unaltered down to 5 K. In order to demonstrate the role of vacancies in the near surface region in generating the ferromagnetic (FM) signal, the MgO crystals are irradiated with 2.5 MeV protons and the FM signal increases by an order of magnitude. The complications introduced by this magnetism of the MgO substrate for the characterization of atomically-thin films is illustrated with Fe/Ni superlattices, where the significant difference in volume between ultrathin films and substrate jeopardizes their magnetic signals when using volume-sensitive techniques, such as SQUID. To ensure an accurate magnetic characterization of atomically-thin films, a surface sensitive magnetometry technique, such as Magneto Optic Kerr Effect (MOKE), that successfully minimizes substrate contributions, has to be employed.

1. Introduction

Years ago it was widely accepted that long range magnetic order in an insulator implies that the cation has to have partially filled d or f electron shells. Stoichiometric bulk MgO with its wide bandgap (7.8 eV), completely filled electron shells and its spin-polarized p band [1] was considered the prototype of a diamagnetic insulator and, as such, it has been widely used as a magnetically inert substrate for the growth of thin films of magnetic materials, including atomically-thin, van der Waals layers [2]. There were, however, reports [3–8] demonstrating that *thin films* of MgO showed ferromagnetism even at 300 K, with relatively large (5.7–150 emu/cm^3) saturation magnetization values, which depend on the temperature of deposition and measurement and on annealing conditions (vacuum, oxygen or hydrogen) [3–8].

These observations were made in the wake of the discovery in 2004 of the so called d^0 magnetism in thin films of undoped oxides, where there were no magnetic ions with open d or f shell, a discovery that challenged our understanding of magnetism in insulators [9–19].

Room temperature ferromagnetism (RTFM) in thin MgO films was assigned to vacancies and other structural defects in the grown films. This was confirmed by Density Functional Theory (DFT) simulations that ascribe RTFM to the presence (and concentration) of Mg vacancies,

* Corresponding authors.
E-mail address: rodolfo.miranda@imdea.org (R. Miranda).

https://doi.org/10.1016/j.jmmm.2026.173986
Received 26 January 2026; Received in revised form 20 February 2026; Accepted 1 March 2026
Available online 10 March 2026

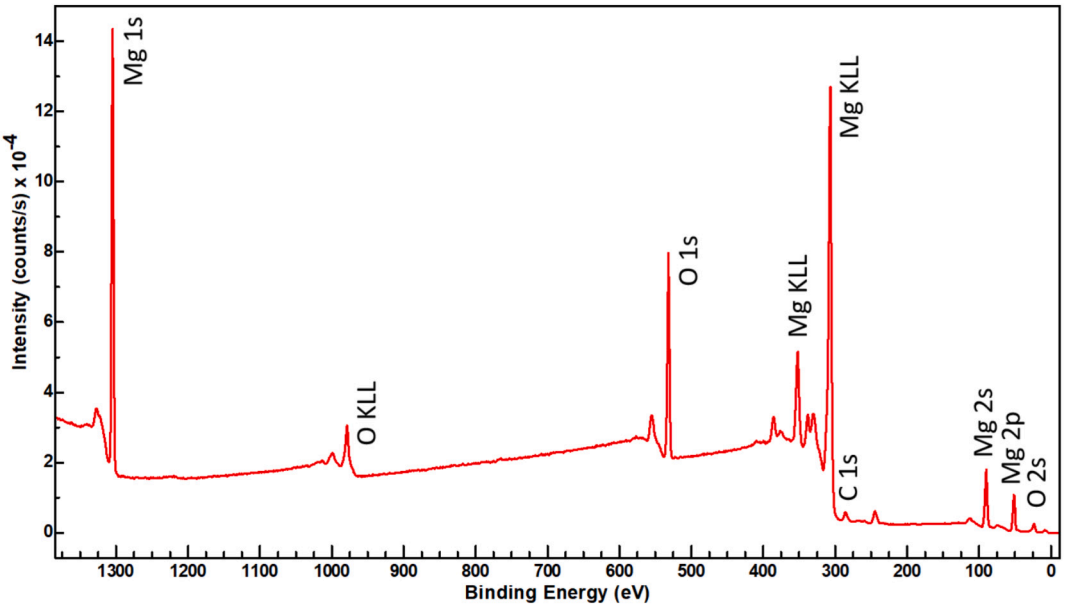

Fig. 1. XPS survey spectrum of a pristine MgO(001) single crystal heated in UHV to 800 °C. No impurities are detected within the sensitivity of XPS. Generally, vacuum annealing is expected to increase the number of oxygen vacancies in the surface region of the sample.

which create free electrons in oxygen ions around the metal vacancies, whose unbalanced magnetic moments can couple ferromagnetically even at 300 K [20–23]. "Perfect" single crystals were still considered as strictly diamagnetic, although a pioneer work raised a warning flag by showing RTFM in a range of single crystals traditionally considered diamagnetic [24] and ferromagnetism (but only below 40 K) was also reported in a MgO single crystal irradiated with neutrons [25].

We demonstrate in the following that, in spite of a widely spread belief, highly perfect MgO(001) single crystals display a ferromagnetic signal even at 300 K that, although small, can mask completely the signal coming from ultrathin magnetic films grown on them and that an accurate magnetic characterization of atomically-thin films requires the use of a surface sensitive magnetometry technique such as MOKE. We further shed light on the origin of the magnetic signal in MgO single crystals. There are two contributions: a paramagnetic signal coming from magnetically isolated impurities in the bulk and a ferromagnetic signal coming from magnetically coupled surface vacancies. The latter can be increased by an order of magnitude by means of controlled proton irradiation, which leaves the former unaffected.

The issue of RTFM in MgO is relevant in practice because bulk MgO single crystals are often used as substrates for the growth of ultrathin magnetic films, superlattices and atomically-thin van der Waals magnetic layers, assuming that their behavior is perfectly diamagnetic, and thus, with no influence in the measured magnetic properties. We illustrate the role of RTFM of MgO by showing that the magnetic properties of an atomically-thin Fe/Ni superlattice with monolayer periodicity are completely masked by the SQUID signal coming from the MgO single crystal substrate.

2. Experimental

MgO(001) single crystals purchased from CRYSTAL GmbH in 20 × 10 × 0.50 mm size were cut with a diamond tip in the desired shape, chemically cleaned with acetone, isopropanol and deionized water in an ultrasonic bath before being mounted in a molybdenum sample holder and inserted into a fast entry chamber connected to the ultra-high vacuum (UHV) chamber. The crystals were cleaned in-situ by annealing at 800 °C in UHV for 15 min to achieve a clean surface.

Irradiation of the MgO pristine sample was done at Centro de Microanálisis de Materiales (CMAM-UAM) using a beam of 2.5 MeV protons. Only half of the sample was exposed, the other one being protected with a shadow mask. The mask was set sufficiently close to the surface as to prevent from edge effects. This allowed us to do v-MOKE magnetometry on each region. The irradiation energy scans promote the creation of vacancies from the surface down to a depth of 35 μm, as estimated using the SRIM calculation software. The total fluency was 1.4×10^{17} ions/cm^2, creating an estimated concentration of oxygen vacancies of $\approx 3.0 \times 10^{21}$ cm^{-3}. Considering that irradiation creates also Mg vacancies in a number of around two thirds of those of oxygen, the total (combined) density of vacancies is $\approx 5.0 \times 10^{21}$ cm^{-3}. This is 4.6% of the atomic density of MgO.

For the growth of the Fe/Ni film the MgO(001) substrates were covered with a 30 nm buffer layer of Ir(100) grown by sputtering using a water-cooled Ir (99.99%) target of 3 in.. The sputtering was carried out with an Ar pressure of 7.4×10^{-3} mbar and a deposition rate of 0.3 Å/s. The MgO(001) substrate was maintained at 600 °C during growth of the Ir(100) buffer layer to optimize its crystalline quality, as checked by X-ray diffraction (XRD) and Low Energy Electron Diffraction (LEED) (see Suppl. Info Fig. S2).

Atomically thin Fe/Ni superlattices with (100) orientation were then grown in the same UHV chamber with a base pressure of 3×10^{-10} mbar via Molecular Beam Epitaxy (MBE) using a four-pocket evaporator that allows the alternate deposition of Fe and Ni atomically- thick monolayers. Finally, a 10 nm V capping layer was grown by MBE at 300 K to protect the samples from the atmosphere for further structural and magnetic analysis outside the growth chamber.

The crystalline structure and thickness of all the components (buffer, Fe/Ni multilayer film, and capping) of the samples were determined by X-Ray Diffraction (XRD) and X-ray reflectivity (XRR) respectively, with a Rigaku diffraction system with a Cu Kα_1 source (1.5405 Å) and the data was analyzed using the Rigaku software. The thickness was also calculated using an X-ray Photoemission Spectroscopy (XPS) system using monochromatized Al Kα X-rays at $h\nu = 1486.6$ eV, which was connected to the growth chamber. To calculate the thickness via XPS, the intensity of the Ir 4f peaks has been measured before and after FeNi growth and, assuming layer-by-layer growth, the FeNi thickness was estimated with the Beer-Lambert law [26].

The magnetic characterization of the samples was performed with a SQUID Quantum Design MPMS XL with EverCool and a vectorial Magneto Optic Kerr Effect (MOKE) magnetomer equipped with a

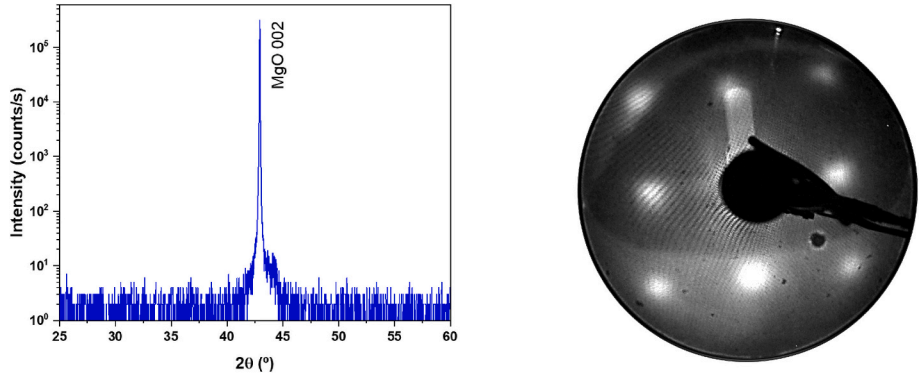

Fig. 2. Left) Wide range X-Ray Diffractogram, from 25 to 60 degrees for a representative MgO(001) single crystal. Only the 002 peak for the MgO substrate is observed. The small shoulder at 44° comes from the sample holder. Right) LEED pattern of MgO(001) recorded at 70 eV.

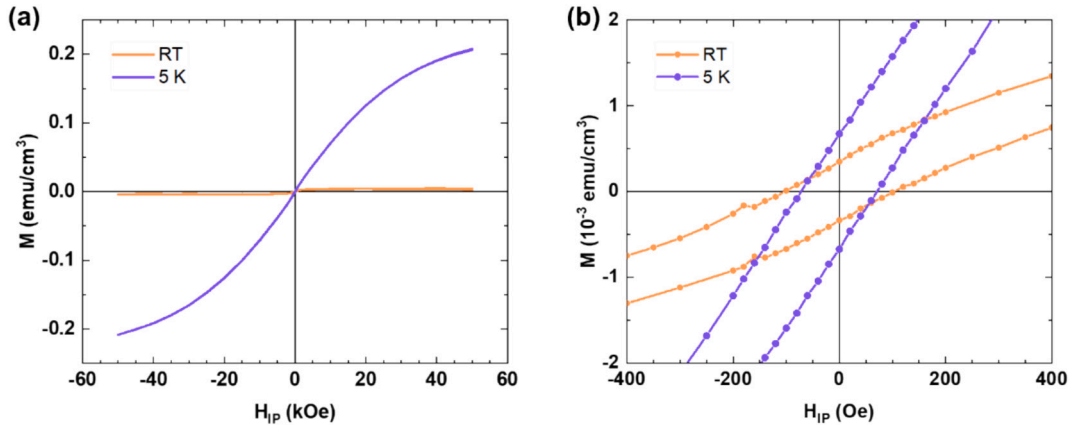

Fig. 3. a) In-plane magnetization curves measured by SQUID at 5 K (blue) and room temperature (red) for a representative pristine MgO(001) single crystal. The magnetic signal has been normalized by the volume of the crystal and reaches a maximum value of 0.24 emu/cm^3 at 5 K with 50 kOe of applied field; b) Blow up of the data at low magnetic fields illustrating the magnetic order hysteresis loops of MgO(001) at 5 K and 300 K. Notice the difference in scale with a). (For interpretation of the references to colour in this figure legend, the reader is referred to the web version of this article.)

cryostat capable of reaching 25 K at the sample. The SQUID characterization has been performed in the In-Plane (IP) and Out-Of-Plane (OOP) directions with a maximum applied field of 50 kOe. The process of demagnetizing the coils has been carried out carefully before every measurement. The MOKE setup only allows for the IP characterization of the sample with an applied field up to 2.5 kOe. Before analyzing the results, the diamagnetic component from the sample holder and the material has been subtracted.

3. Results and discussion

3.1. MgO(001) single crystals

The X-ray photoelectron spectroscopy (XPS) compositional analysis of the ≈20 nm closer to the surface of the MgO(001) single crystal heated in UHV at 800 °C to clean the surface is shown in Fig. 1. The binding energies (BE) of the peaks have been consistently determined by aligning the C 1 s peak position to 284.7 eV. Only Mg and O core levels (and Auger transitions) are seen. No impurities have been detected within the sensitivity of XPS (0.1%). The composition of the near surface region, obtained from the ratio of Mg2s and O2s peaks (with photoelectrons of similar energy, i.e. similar mean free path) indicates an atomic ratio of Mg:O substantially larger than 1:1; the larger fraction of Mg (59 ± 2%) being consistent with the presence of ≈10% oxygen vacancies generated by the annealing in UHV in the ≈10 nm-deep surface region tested by XPS.

The left part Fig. 2 shows the X-Ray Diffraction pattern indicating that the MgO single crystal is (001) oriented with a lattice parameter a = 4.212 Å and an apparent crystallite size (≈155 nm) limited by the resolution of the XRD spectrometer. The surface crystallinity and orientation of MgO is confirmed by the Low Energy Electron Diffraction (LEED) pattern reproduced on the right side of the figure.

Fig. 3a shows the In Plane (IP) magnetization curves measured at 300 K and 5 K for pristine MgO(001), where the magnetization has been normalized to the volume of the sample. At 5 K, the IP magnetization shows a strong increase with respect to the one at 300 K due to a strong paramagnetic contribution. The emergence of this new signal only at 5 K is due to the temperature dependence of the magnetic susceptibility, which is inversely proportional to temperature for paramagnetic materials; accordingly, the paramagnetic signal is much higher at 5 K than at 300 K. A blow up of the data at low fields shown in Fig. 3b reveals also magnetic order at *both* 5 K and 300 K with similar remanence (≈ 3–6 × 10^{-4} emu/cm^3) and similar coercive fields (71 Oe at 5 K and 103 Oe at 300 K).

The magnetism of the pristine MgO(001) single crystal is quite small, since saturation magnetization at 300 K is only 3 × 10^{-3} emu/cm^3, whilst at 5 K the magnetization at 50 kOe is 0.24 emu/cm^3 (see Fig. 3), which are 3.2 × 10^5 and 5.4 × 10^3 times smaller than the saturation magnetization of standard FM metals (e.g. 1270 emu/cm^3 for FeNi, see below), at 300 and 5 K, respectively. Although a bulk, perfectly stoichiometric MgO single crystal is expected to be strictly diamagnetic [1], it is well known that thin films of MgO can develop d^0 ferromagnetism even at 300 K due to defects or impurities [3–8]. It is essential to note that the tiny magnetization at 300 K of single crystals of MgO() observed

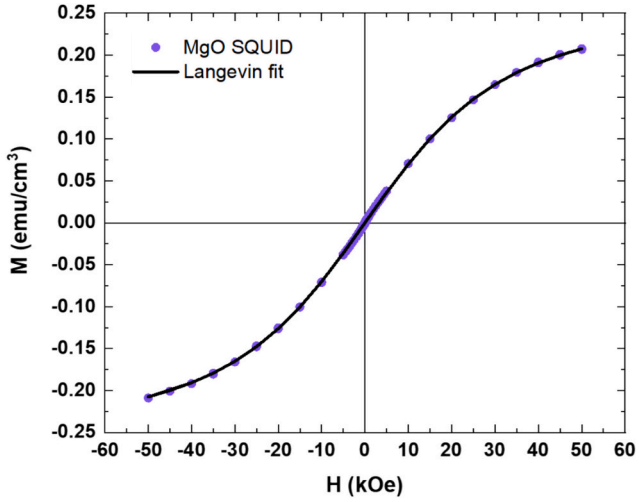

Fig. 4. Experimental magnetization curve for MgO(001) single crystal at 5 K fitted to the Langevin function.

here is three orders of magnitude smaller than usually reported for MgO thin films deposited at 300 K (5.7 emu/cm^3 [4], 8 emu/cm^3 [5], 15 emu/cm^3 [6], 8.57 emu/cm^3 [7]). For MgO films deposited at 200 °C, it has been reported that the magnetization decreases to 0.4 emu/cm^3 [5], still hundred times larger than reported here.

To trace the origin of the anomalously high magnetization values at 5 K, the magnetization curve of Fig. 3a has been fitted with the classical Langevin model for paramagnetism given in eq. 2.

$$M = n\mu(\coth(\mu B/k_B T) - (k_B T/\mu B)) \quad (1)$$

where n is the density of magnetic objects, μ is the magnetic moment per object, B is the applied magnetic field, and T the temperature. The fitting with $1/k_B T = 1.44859 \times 10^{22}$ is shown on Fig. 4.

The fitting yields an average magnetic moment per magnetic object of $\mu = 5.42 \times 10^{-23}$ J/T = 5.85 μ_B, which implies the presence of paramagnetic clusters. Paramagnetic clusters with larger magnetic moments (12.9–22.5 μ_B), have been observed in muon irradiated ZnO rods [18]. From the fit to the Langevin function it is possible to extract the concentration of magnetic clusters in the bulk of the MgO(001) sample with a value of 5.13×10^{18} clusters/cm^3, i.e. ≈ 50 ppm. The corresponding saturation magnetization for this density of magnetic objects would be 0.27 emu/cm^3, in good agreement with the value of 0.24 emu/cm^3 measured at 5 K and 50 kOe. The nature of these paramagnetic clusters cannot be defined precisely. We can tentatively ascribe them to magnetic impurities below the detection level of XPS (0.1%), introduced in the crystal by the growth method. In fact, we have found by X-Ray Fluorescence (XRF) that the single crystals of MgO contain magnetic ions in concentrations of the same order of magnitude (Fe ≈ 1.9×10^{19} cm^{-3}, V ≈ 3.5×10^{18} cm^{-3}, Mn ≈ 2.2×10^{18} cm^{-3}) than the one obtained here. This is in agreement with previous reports that single crystals of MgO contain magnetic ions in similar concentrations (Fe = 3.4×10^{18} cm^{-3}, Cr = 1.1×10^{18} cm^{-3}, V = 1.5×10^{18} cm^{-3}, Mn = 0.5×10^{18} cm^{-3}) [24].

On the contrary, the small ferromagnetic (FM) signal observed in Fig. 3 at 300 K can be assigned to d^0 ferromagnetism in MgO produced by a much higher concentration of intrinsic vacancies at the surface region, in agreement with the assignment to Mg vacancies of the FM signals observed at 300 K on MgO deposited films [3–8]. The saturation magnetization of MgO single crystals at 300 K, however, is 3×10^{-3} emu/cm^3, i.e. 100 times smaller than the one at 5 K and three to five orders of magnitude smaller than the signal on thin deposited films. Spin-polarized ab-initio calculations show that neutral Mg vacancies are responsible for d^0 ferromagnetism in this material with Curie temperature well above 300 K [3,20–23]. According to most calculations, Mg vacancies can induce local moments in MgO, while O vacancies cannot, irrespective of the concentration [20]. The spin polarization of 2p electrons of oxygen atoms adjacent to the Mg vacancy is responsible for the induced magnetic moments as concluded from X-ray magnetic circular dichroism [3]. Calculations have indicated that a concentration of vacancies of the order of 9.3% results in magnetic moments of the order of 4.7 μ_B [20,21]. If we assume that the magnetic moment of the objects generating the ferromagnetic signal is of this order of magnitude, their concentration would be ≈ 5 × 10 [16] cm^{-3}. If they are mostly located in a depth of ≈ 20 nm at the surface of the crystal (sampled by XPS), this corresponds to ≈ 10 at. % of vacancies in the surface region. This is perfectly consistent with the imbalance between Mg and O detected by XPS after heating the pristine sample in UHV.

Notice that the formation of localized magnetic moments does not necessarily lead to collective magnetism. To promote ferromagnetism, both a concentration of defects large enough for magnetic percolation and an appropriate interaction should be granted.

In order to verify that a large density of composite vacancies in the surface region is responsible for the ferromagnetic signal in pristine MgO single crystals at 300 K, we have irradiated a MgO(001) single crystal with 2.5 MeV protons to a total dose of 1.4×10^{17} cm^{-2}. The irradiation causes the appearance of defects within a region ≈ 35 μm-deep close to the surface of the crystal. The calculated density of Mg and O vacancies introduced is ≈ 5×10^{21} cm^{-3}, i.e. ≈ 4.6% of the atomic density of MgO (1.07×10^{23} cm^{-3}). The magnetic characterization by SQUID at 5 K and

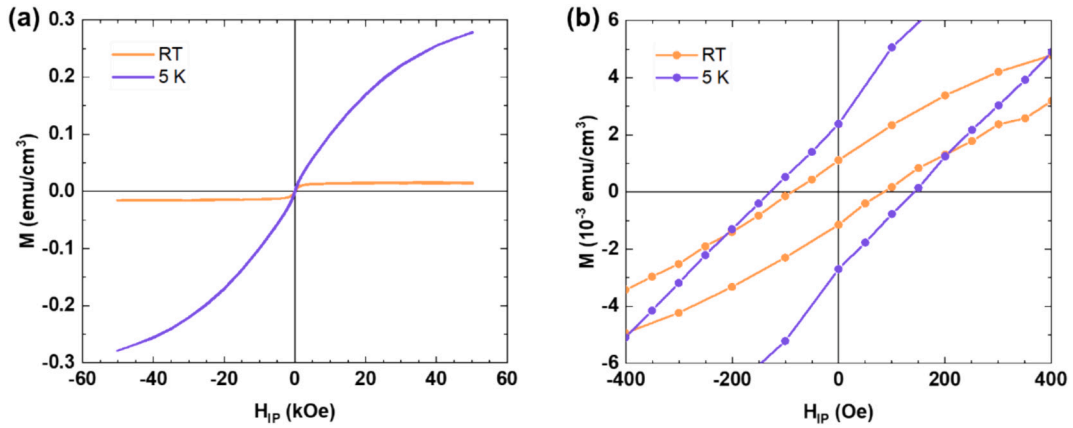

Fig. 5. Magnetization curves measured by SQUID in-plane at room temperature (orange) and 5 K (purple) for a MgO(001) single crystal irradiated with 2.5 MeV protons The magnetic signal has been normalized by the volume of the crystal. (For interpretation of the references to colour in this figure legend, the reader is referred to the web version of this article.)

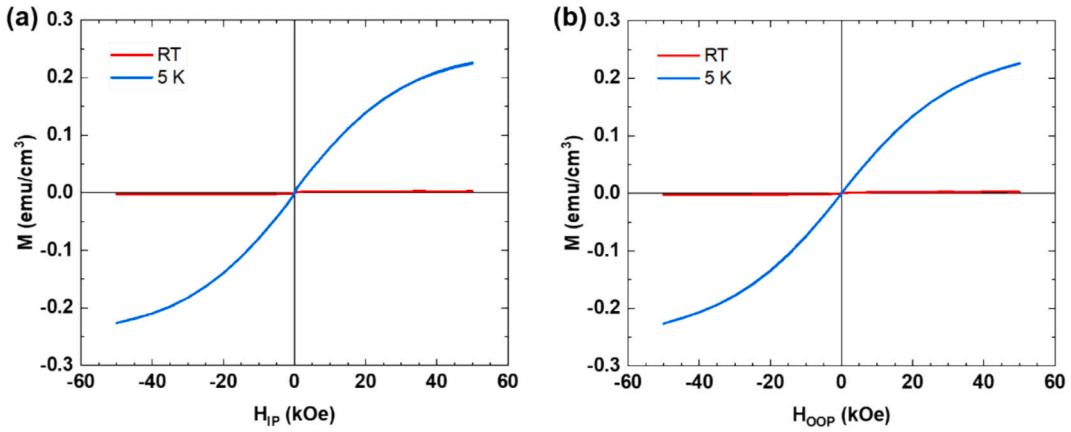

Fig. 6. Comparison between room temperature (red) and 5 K (blue) hysteresis loops of a 1.2 nm-thick FeNi/Ir(100)/MgO(001) sample measured by SQUID and normalized by the total volume of the sample (a) in-plane and (b) out-of-plane. (For interpretation of the references to colour in this figure legend, the reader is referred to the web version of this article.)

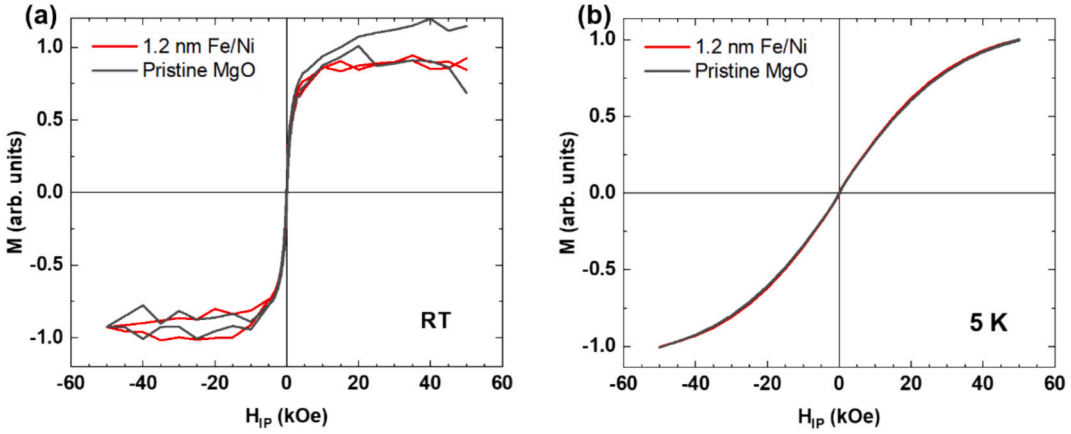

Fig. 7. Direct comparison between in-plane hysteresis cycles of the pristine MgO(001) single crystal and the 1.2 nm-thick FeNi/MgO(001) film at (a) room temperature and (b) 5 K. Both magnetization curves are normalized to 1 to illustrate their similarity.

room temperature is shown on Fig. 5. A strong paramagnetic signal is detected at 5 K with a saturation magnetization of 0.24 ± 0.04 emu/cm^3, essentially identical to the one before irradiation and reported in Fig. 3. The corresponding Langevin fit indicates that average magnetic moment and density of the paramagnetic impurities is unchanged with respect to the observation before irradiation. This suggests that the paramagnetic signal dominating at 5 K originates in the bulk impurities detected by X-ray Fluorescence and mentioned above, whose concentration is not affected by the proton irradiation.

The FM signal, on the contrary, is much stronger than before the irradiation. The saturation magnetization at 300 K of the FM signal is 1.5×10^{-2} emu/cm^3, i.e. 10 times larger than before the irradiation. The remanence is also an order of magnitude larger than before irradiation, while the temperature dependence of both remanence (2×10^{-3} emu/cm^3 at 5 K and 1×10^{-3} emu/cm^3 at 300 K) and coercivity (135 Oe at 5 K and 87 Oe at 300 K) is rather weak. This increase in the FM signal upon proton irradiation further suggests that the FM signal comes from the additional structural/compositional defects introduced in the surface region by the irradiation process.

3.2. *Atomically-thin Fe/Ni superlattices with monolayer periodicity*

Since we have shown that even a highly perfect, single crystal of MgO (001) can develop a small, but measurable ferromagnetic signal, it is important to consider whether this signal could jeopardize the magnetic characterization of atomically thin films often deposited on MgO substrates. To illustrate this point, we have chosen atomically-thin Fe/Ni superlattices with monolayer periodicity, an epitaxial system that has attracted considerable attention recently, because it is considered a model system for the $L1_0$ FeNi bulk phase, a promising powerful magnet without rare earths [27–29].

Fig. 6 shows that for an atomically (1.2 nm) thick Fe/Ni superlattice consisting of 3 double atomic planes of Fe and Ni in a (100) orientation, a strong paramagnetic signal is detected at 5 K with a saturation magnetization of 0.23 emu/cm^3, identical to the one measured without the Fe/Ni film. Also at 300 K both In-Plane and Out-Of-Plane signals are completely dominated by the ferromagnetic signal from the MgO substrate.

In fact, as Fig. 7 demonstrates, the SQUID signal from the 1.2 nm Fe/Ni superlattice is *indistinguishable* from the one without the Fe/Ni film both at 300 K and at 5 K. The large substrate/film volume ratio ($V_{MgO}/V_{FeNi} = 4.2 \times 10$ [5]) and the strong signal from the MgO substrate completely overwhelms the magnetic signal coming from the Fe/Ni ultrathin film. Obviously for much thicker magnetic films (see Suppl. Info. Fig. S3), their SQUID signal finally dominates the one coming from the substrate, but one should note that in order to determine the thickness limit from which the intrinsic magnetic properties of the films dominate the measurements, a *previous* determination of the magnetic signal coming from the MgO substrate is required.

The solution to detect the signal coming from atomically thin

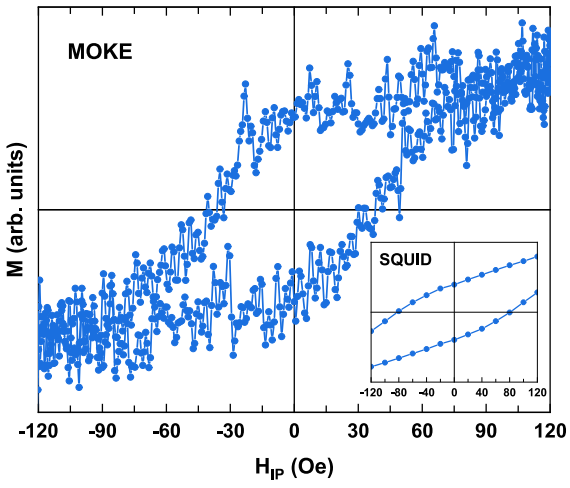

Fig. 8. In-plane hysteresis loops of a 1.2 nm-thick FeNi/ Ir(100)/ MgO(001) film measured by Magneto-Optic Kerr Effect (MOKE) magnetometry at 25 K. The inset shows the SQUID measurement of the same sample at 5 K.

magnetic film is relying only on surface-sensitive magnetometry techniques, such as MOKE, which is sensitive to the penetration depth of the laser used, typically around 20–40 nm.

Fig. 8 shows the MOKE results for the 1.2 nm-thick film of Fe/Ni (i.e. 3 bilayers of the atomic periodicity Fe/Ni superlattice), where a ferromagnetic hysteresis loop with a coercivity of 36 Oe can be observed. This result is clearly different from the hysteresis loop of the same sample measured with SQUID reproduced in the inset, where the apparent coercivity is much higher and the shape of the loop is strongly affected by the ferromagnetic contribution of the MgO single crystal underneath. Hence, MOKE measurements, because they are only sensitive to a few nanometers below the surface, allow for a true magnetic characterization of ultrathin magnetic films without receiving magnetic signal from the MgO substrate.

4. Conclusions

In conclusion, even highly perfect and presumably diamagnetic substrates, such as MgO single crystals, which are used routinely as substrates for the growth of ultrathin magnetic films or in the shape of thin films as tunneling barriers, may present a small, but detectable, defect-related ferromagnetic signal that can easily mask the intrinsic magnetic properties of atomically thin films deposited on them when the magnetic measurements are based on bulk sensitive techniques, such as SQUID. Since the magnetic signal from the MgO depends on the specific number of vacancies in the substrate, a prior careful magnetic characterization of the substrates employed to grow ultrathin magnetic films is mandatory. An alternative magnetic characterization of the ultrathin films based on surface sensitive techniques, such as MOKE, is required.

CRediT authorship contribution statement

Iban Llamas: Formal analysis, Data curation. **José Luis Fernández-Cuñado:** Methodology, Formal analysis, Data curation. **Cristina Navío:** Supervision, Methodology. **Pilar Marín:** Data curation. **Patricia de la Presa:** Data curation. **Rodolfo Miranda:** Writing – review & editing, Writing – original draft, Supervision, Funding acquisition, Conceptualization. **Antonio Hernando:** Validation, Supervision, Formal analysis, Conceptualization.

Declaration of competing interest

The authors declare that they have no known competing financial interests or personal relationships that could have appeared to influence the work reported in this paper.

Acknowledgements

The research was supported by the “Severo Ochoa” Programme for Centres of Excellence in R&D (CEX2020-001039-S) and by the Regional Government of Madrid through NANOMAGCOST (S2018/NMT-4321) and Mag4TIC-CM (TEC-2024/TEC-380) projects. We acknowledge partial financial support through a collaboration project between Robert Bosch GmbH and IMDEA Nanociencia. We thank Dr. Juan Cabanillas for help with the photoluminescence measurements.

Appendix A. Supplementary data

Supplementary data to this article can be found online at https://doi.org/10.1016/j.jmmm.2026.173986.

Data availability

Data will be made available on request.

References

[1] U. Schonberger, F. Aryasetiawan, Bulk and surface electronic structures of MgO, Phys. Rev. B 52 (1995) 8788.
[2] For a collection of review papers on the growth of metallic magnetic ultrathin films see J. Physics: Condes. Matter 11 (48), 9365 (1999) For recent work on 2D magnetic materials see M. Gibertini, M. Koperski, A.F. Morpurgo, K.S. Novoselov, Magnetic 2D materials and heterostructures, Nat. Nanotechnol. 14 (2019) 408–419.
[3] C. Martínez-Boubeta, J.I. Beltrán, Ll. Balcells, Z. Konstantinović, S. Valencia, D. Schmitz, J. Arbiol, S. Estrade, J. Cornil, B. Martínez, Ferromagnetism in transparent thin films of MgO, Phys. Rev. B 82 (2010) 024405.
[4] C.M. Araujo, M. Kapilashrami, X. Jun, 0.D. Jayakumar, S. Nagar, Y. Wu, C. Arhammar, B. Johansson, L. Belova, R. Ahuja, G.A. Gehring, K.V. Rao, Room temperature ferromagnetism in pristine MgO thin films, Appl. Phys. Lett. 96 (6) (2010) 232505.
[5] Jing Li, Y. Jiang, Yong Li, Deren Yang, Y. Xu, Mi Yan, Origin of room temperature ferromagnetism in MgO films, Appl. Phys. Lett. 102 (2013) 072406.
[6] S.K. Mahadeva, J. Fan, A. Biswas, G.M. Rao, K.S. Sreelatha, L. Belova, K.V. Rao, A comparative study of room temperature ferromagnetism in MgO films deposited by rf/dc sputtering using high purity Mg and MgO targets, Mater. Express 3 (4) (2013) 327.
[7] J. Li, Y. Jiang, G. Bai, T. Ma, D. Yang, Y. Du, M. Yan, Room temperature ferromagnetism of amorphous MgO films prepared by pulsed laser deposition, Appl. Phys. A Mater. Sci. Process. 115 (2014) 997–1001.
[8] J. Pal Singh, Keun Hwa Chae, d0 ferromagnetism of magnesium oxide, Condens. Matter 2 (2017) 36.
[9] I.S. Elfimov, S. Yunoki, G.A. Sawatzky, Possible path to a new class of ferromagnetic and half-metallic ferromagnetic materials, Phys. Rev. Lett. 89 (2002) 216403.
[10] M. Venkatesan, C.B. Fitzgerald, J.M.D. Coey, Thin films: unexpected magnetism in a dielectric oxide, Nature 430 (2004) 630.
[11] J.M.D. Coey, M. Venkatesan, P. Stamenov, C.B. Fitzgerald, L.S. Dorneles, Magnetism in hafnium dioxide, Phys. Rev. B 72 (2005) 024450.
[12] S.D. Yoon, Y. Chen, T.L. Goodrich, X. Zuo, D.A. Arena, K. Ziemer, C. Vittoria, V. G. Harris, Oxygen-defect-induced magnetism to 880 K in semiconducting anatase TiO2-δ films, J. Phys. Condens. Matter 18 (2006) L355.
[13] M.A. Garcia, J.M. Merino, E.F. Pinel, A. Quesada, J. de la Venta, M.L.R. Gonzalez, G.R. Castro, P. Crespo, J. Llopis, J.M. Gonzalez-Calbet, A. Hernando, Magnetic properties of ZnO nanoparticles, Nano Lett. 7 (2007) 1489.
[14] Q. Xu, H. Schmidt, S. Zhou, K. Potzger, M. Helm, Room temperature ferromagnetism in ZnO films due to defects, Appl. Phys. Lett. 92 (2008) 082508.
[15] Q. Wang, Q. Sun, G. Chen, Y. Kawazoe, P. Jena, Vacancy-induced magnetism in ZnO thin films and nanowires, Phys. Rev. B 77 (2008) 205411.
[16] D. Mishra, P. Kumar, M.K. Sharma, J. Das, S. Singh, B. Roul, S. Varma, R. Chatterjee, V. Srinivasu, D. Kanjilal, Ferromagnetism in ZnO single crystal, Phys. B Condens. Matter 405 (2010) 2659–2663.
[17] H. Zhang, W. Li, G. Qin, H. Ruan, D. Wang, J. Wang, C. Kong, F. Wu, L. Fang, Surface ferromagnetism in ZnO single crystal, Solid State Commun. 292 (2019) 36–39.
[18] C. Landry, A. Morrison, M. Esmaeili, K. Ghandi, Muon irradiation of ZnO rods: superparamagnetic nature induced by defects, Nanomaterials 12 (2022) 184.
[19] N.H. Hong, N. Poirot, J. Sakai, Ferromagnetism observed in pristine SnO2 thin films, Phys. Rev. B 77 (2008) 033205 [12] J. M. D. Coey, Magnetism in d^0 oxides, Nature Materials **18**, 652-656 (2019).
[20] F. Wang, Z. Pang, Liang Lin, S. Fang, Y. Dai, Shenghao Han, Magnetism in undoped MgO studied by density functional theory, Phys. Rev. B 80 (2009) 144424.

[21] Feng Gao, Jifan Hua, Chuanlu Yangb, Y. Zhenga, H. Qin, Li Suna, Xiangwei Konga, Minhua Jiang, First-principles study of magnetism driven by intrinsic defects in MgO, Solid State Commun. 149 (2009) 855.
[22] F.-G. Kuang, Shu-Ying Kang, Xiao-Yu Kuang, qi-Feng Chenb, An *ab initio* study on the electronic and magnetic properties of MgO with intrinsic defects, RSC Adv. 4 (2014) 51366.
[23] Min Wang, S. Tang, D. Hou, F. Meng, Y. Han, J. Ren, B. Wang, Tiege Zhou, Possible origin of ferromagnetism in pristine magnesium oxide film, Physica 590 (2020) 412214.
[24] M. Khalid, A. Setzer, M. Ziese, P. Esquinazi, D. Spemann, A. Pöppl, E. Goering, Ubiquity of ferromagnetic signals in common diamagnetic oxide crystals, Phys. Rev. B 81 (2010) 214414.
[25] M. Cao, Y. Ma, X. Wang, C. Ma, W. Zhou, X. Wang, W. Tan, J. Du, Point defects and magnetic properties of neutron irradiated MgO single crystal, AIP Adv. 7 (2017) 5.
[26] R. Paynter, An arxps primer, J. Electron Spectrosc. Relat. Phenom. 169 (2009) 1–9.
[27] T. Shima, M. Okamura, S. Mitani, K. Takanashi, Structure and magnetic properties for $L1_0$-ordered FeNi films prepared by alternate monatomic layer deposition, J. Magn. Magn. Mater. 310 (2007) 2213–2214.
[28] M. Kotsugi, M. Mizuguchi, S. Sekiya, M. Mizumaki, T. Kojima, T. Nakamura, H. Osawa, K. Kodama, T. Ohtsuki, T. Ohkochi, K. Takanashi, Y. Watanabe, Origin of strong magnetic anisotropy in $L1_0$-FeNi probed by angular-dependent magnetic circular dichroism, J. Magn. Magn. Mater. 326 (2013) 235–239.
[29] J. Marciniak, M. Werwiński, Magnetic anisotropy of $L1_0$ FeNi (001), (010), and (111) ultrathin films: a first-principles study, J. Magn. Magn. Mater. 609 (2024) 172455.